

## Silica-based Composite Membranes for Methanol Fuel Cells Operating at High Temperature

A. Alvarez<sup>1</sup>, C. Guzman<sup>1</sup>, C. Peza-Ledesma<sup>2</sup>, Luis A. Godinez<sup>1</sup>, R. Nava<sup>2</sup>, S.M. Duron-Torres<sup>3</sup>,  
J. Ledesma-Garcia<sup>2,\*</sup> and L.G. Arriaga<sup>1</sup>

<sup>1</sup>Centro de Investigación y Desarrollo tecnológico en Electroquímica, Parque Tecnológico Querétaro, Sanfandila, Pedro Escobedo, C. P. 76703 Querétaro, México.

<sup>2</sup>División de Investigación y Posgrado, Facultad de Ingeniería, Universidad Autónoma de Querétaro, Cerro de las Campanas S/N, C. P. 76010 Querétaro, México.

<sup>3</sup>UACQ-UAZ, CU Siglo XXI-Edificio 6, Km. 6 Carr. Zac.-Gdl., La Escondida, Zacatecas, Zac. C.P. 98160, México.

Received: November 30, 2010, Accepted: February 01, 2011, Available online: April 07, 2011

**Abstract:** In this work, composite membranes were prepared from a mixture of Nafion<sup>®</sup> ionomer with mesoporous (SBA-15) and microstructured silica (SiO<sub>2</sub>). The silica-based materials were synthesized using the sol-gel technique and their properties were characterized by TEM, BET, SEM and XRD. A glass cell with two chambers was used to evaluate the permeability of methanol of the composite membranes and its performance was compared with a commercial Nafion 115 membrane. The composite membranes showed smaller value of methanol permeability (around 19%) than that obtained when was used a commercial membrane. In terms of the fuel cell performance, the composite membranes showed a larger maximum power density (62 and 29 mWcm<sup>-2</sup> for the SiO<sub>2</sub> and SBA-15 composite membrane respectively) than that obtained for the commercial membrane at high temperature conditions (100°C).

**Keywords:** composite membrane, NafionDMFC, High temperature DMFC

### 1. INTRODUCTION

Direct methanol fuel cells (DMFCs) have received the attention as an alternative energy source for a wide range of applications; particularly for portable power sources since its liquid-fuelled system involves an easy manipulation as well as a low environmental impact [1-5]. Nafion membranes on the other hand, constitute a well known proton exchange system for DMFC systems due to its convenient electrochemical, mechanical and thermal stability and high proton conductivity properties [4]. However, the main problems currently associated to the direct methanol fuel cell technology are the following: (1) the anode reaction has poor electrode kinetics, particularly at low temperatures, making highly desirable to improve the performance of catalysts at high temperatures; (2) the permeability and the poor stability of the perfluorosulfonic acid membranes in the presence of methanol, which resides in the crossover phenomenon; and (3) at high temperature, in order to overcome the limitations in the anode kinetics, it is mandatory to

diminish the membrane degradation and to avoid the methanol diffusion to the cathodic compartment [6].

In this context, intensive efforts in order to decrease the methanol crossover are focused mainly on the development of new polymer electrolyte membranes. The incorporation of inorganic oxide particles into Nafion<sup>®</sup> matrix, improves the membranes performance on water uptake, ion-exchange capacity and the operation temperature of the system [7-8].

In this work, Nafion<sup>®</sup> polymer was modified by means of the incorporation of inorganic oxides with different structural properties (SBA-15 and SiO<sub>2</sub>), both prepared by sol-gel method in order to increase the proton conductivity at high temperature of fuel cell and to contribute decrementing the methanol crossover effect. SBA-15 is a mesostructured porous silica with a high surface area and hexagonal arrangement of uniform pores [9-10]. SiO<sub>2</sub> also was synthesized in house resulting in a microstructured porous silica. Preliminary results of water uptake, ion-exchange capacity, methanol permeability and cell performance of the Nafion/SiO<sub>2</sub> and Nafion/SBA-15 composite membrane are presented.

\*To whom correspondence should be addressed: Email: janet.ledesma@uaq.mx

## 2. EXPERIMENTAL

### 2.1. Synthesis of inorganic fillers

Silica (SiO<sub>2</sub>) was synthesized using the sol-gel method under acidic conditions. A tetraethyl-orthosilicate precursor was used (TEOS 98%, Aldrich) and nitric acid (HNO<sub>3</sub>) was utilized as catalyst. An Alcohol/alkoxide molar ratio solution was kept under stirring for 20 minutes. An Water/acid molar ratio solution remained under constant stirring for 5 minutes. Both solutions were mixed at room temperature to form a solid. The resulting material was treated using a tubular furnace (Barnstead Thermolyne) at 150 °C for 2 h to remove residual alcohol and to obtain the silicon oxide [11-12].

For the synthesis of the SBA-15 material, the copolymer Pluronic P123 (EO20PO70EO20, BASF) dissolved in 4M HCl was used as the structure directing agent. TEOS was added to the solution and stirred at 35 °C for 24 h. The resulting solution was transferred into polypropylene bottles and heated at 80 °C for 24 h. The solid product was filtered, washed with deionized water and dried at room temperature for 24 h. In a following stage, the product was heated at 110 °C for 18 h and later kept at 500 °C for 6 h to remove the surfactant [13-15].

### 2.2. Preparation of Composite Membranes

The composite membranes were prepared from 5% Nafion® solution (ElectroChem. Inc.) mixed with 3 % wt. of the relevant inorganic filler and dispersed in an ultrasonic bath for 10 minutes. The resulting solutions were transferred to a dish (10 cm of diameter) and evaporated in an oven (Thermo Scientific) at 100 °C for 1 h until a dense polymer film was obtained [1,16]. Finally, a thermic treatment in boiling 3% H<sub>2</sub>O<sub>2</sub> and 0.5M H<sub>2</sub>SO<sub>4</sub> was accomplished, in order to clean and activate the composite membranes respectively.

### 2.3. Physicochemical characterization of inorganic fillers

The textural properties of inorganic fillers were analyzed by means of adsorption-desorption isotherms of N<sub>2</sub> at 77 K using a Micromeritics TriStar 3000 apparatus. The surface area was calculated according to the Brunauer-Emmett-Teller (BET) Equation. The inorganic fillers were also characterized by X-ray diffraction performed on a Philips diffractometer (PW3710). Yet, infrared spectra (FT-IR) were obtained using a Bruker (Vector 33) spectrophotometer. Spectroscopic data were collected in the range of 400 to 4000 cm<sup>-1</sup>.

### 2.4. Composite Membranes Characterization

#### 2.4.1. Water Uptake (Wup)

Water uptake (Wup %) was determined by the ratio between the weight of wet and dry membrane, by using the equation (1):

$$Wup\% = \left( \frac{W_{wet} - W_{dry}}{W_{dry}} \right) 100 \quad (1)$$

The dry mass was calculated maintaining the samples in an oven under vacuum at 80 °C for 2 h. For wet mass assesment, the samples were immersed in deionized H<sub>2</sub>O at room temperature for 24 h, dipped and weighted [10, 17].

#### 2.4.2. Ion Exchange Capacity (IEC)

In order to determinate the ion exchange capacity, the composite membranes, previously dried, were introduced into a solution of 1M NaCl for 24 h at room temperature. Later, the membranes were titred with a 0.01M NaOH solution [18] to neutralize the exchanged H<sup>+</sup>. Taking into account the dry weight of each sample and plotting the pH variation with the added titrant volume, the NaOH concentration at the equivalent point was determined.

### 2.5 Electrochemical characterization

#### 2.5.1 Measurement of methanol permeability

A two-compartment glass cell with 3.4 mL of volume was used to investigate the methanol permeability through composite membranes at 25 °C. Whereas the compartment I was filled with an aqueous solution containig 1M methanol in 0.5M H<sub>2</sub>SO<sub>4</sub>, the compartment II contained only 0.5M H<sub>2</sub>SO<sub>4</sub> solution. The membrane was clamped between the two compartments and the contents of both were stirred during the experiments. The methanol concentration in compartment II was monitored by chronoamperometry technique [19]. A constant potential ,0.68V vs. the reference electrode Ag/AgCl, was applied during 150 min in a BAS-Epsilon potentiostat (From Bionalytical Systems). A Pt micro-electrode served as working electrode (WE), Ag/AgCl as reference and a Pt wire as a conunter electrode (CE). From the concentration of methanol at any time, it was possible to estimate the methanol permeability (P) using equation (2):

$$C_{II} = \frac{A}{V_{II}} \frac{DK}{L} C_I t \quad (2)$$

Where C<sub>II</sub> is the methanol concentration in compartment II, C<sub>I</sub> is the methanol concentration in compartment I, A and L are the area and thickness of the membrane respectively, D and K are the methanol diffusivity and the partition coefficient between the membrane and the adjacent solution, t is the permeation time, and V<sub>II</sub> is the volume of the solution in compartment II. The DK product corresponds to the methanol permeability P.

#### 2.5.2. Fuel cell performance

Fuel cell performance tests were carried out using a comercial 5 cm<sup>2</sup> fuel cell (Electrochem Inc.) using the composite membranes. The membrane-electrode assemblies were prepared using 2 mg cm<sup>-2</sup> of Pt-Ru (50% wt., Alfa Aesar) for the anode and 1 mg cm<sup>-2</sup> of Pt/C (30% wt. Alfa Aesar) for the cathode. Carbon cloth (GDL ELAT from E-TEK) was used as gas diffusion layer. Direct methanol fuel cell was operated with 2 M MeOH aqueous solution at 8 mL min<sup>-1</sup> of flow rate and fully humidified oxygen was entered in the cathodic compartment at 200 mL min<sup>-1</sup> of flow rate. The back pressure was 30 psi in both anode and cathode. Fuel cell measurements were made using a CompuCell Fuel Cell Test System. The operation temperature of the fuel cell was fixed at 80 and 100 °C.

## 3. RESULTS AND DISCUSSION

### 3.1. Characterization of inorganic fillers

The textural properties of the inorganic fillers are presented in Table 1. Inspection of the data in Table 1 shows that specific surface area and pore diameter values are different for the two silica-based materials, 1039 m<sup>2</sup>g<sup>-1</sup> and 4nm for SiO<sub>2</sub> and 932 m<sup>2</sup>g<sup>-1</sup> and

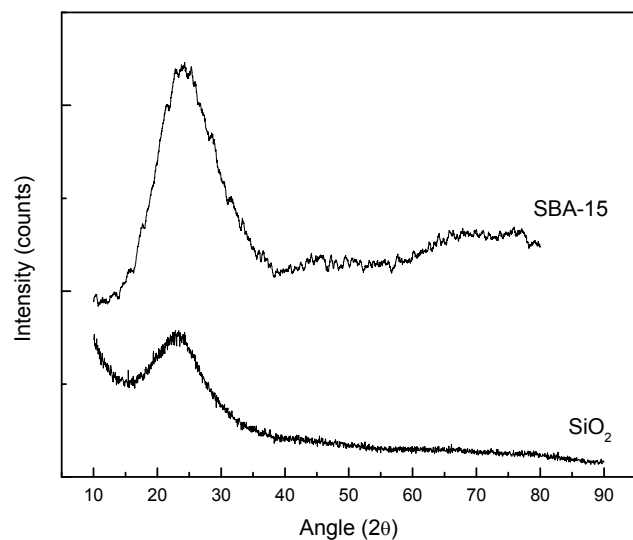


Figure 1. X-ray diffraction patterns of inorganic fillers.

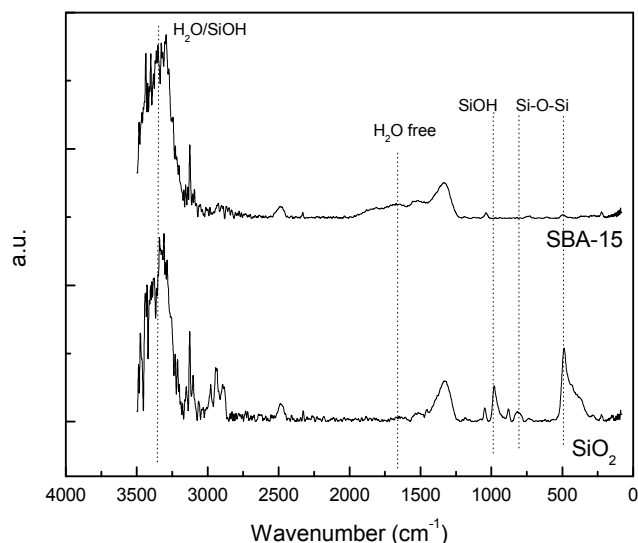


Figure 2. Representative FT-IR spectra of inorganic fillers.

6nm SBA-15, respectively.

X-ray diffraction patterns of SiO<sub>2</sub> and SBA-15 materials are shown in Figure 1 where a broad reflection centered at about 2θ = 24° characteristic of amorphous silica (SiO<sub>2</sub>), can be observed [20].

The FT-IR spectra of the inorganic fillers are shown in Figure 2, in which a typical spectrum of silica (SiO<sub>2</sub>) can be identified. The bands at 811 and 1087 cm<sup>-1</sup> correspond to the symmetric and asym-

Table 1. Textural properties of inorganic fillers.

Inorganic filler	Surface area /m <sup>2</sup> g <sup>-1</sup>	Pore diameter/nm
SiO <sub>2</sub>	1039	4
SBA-15	932	7

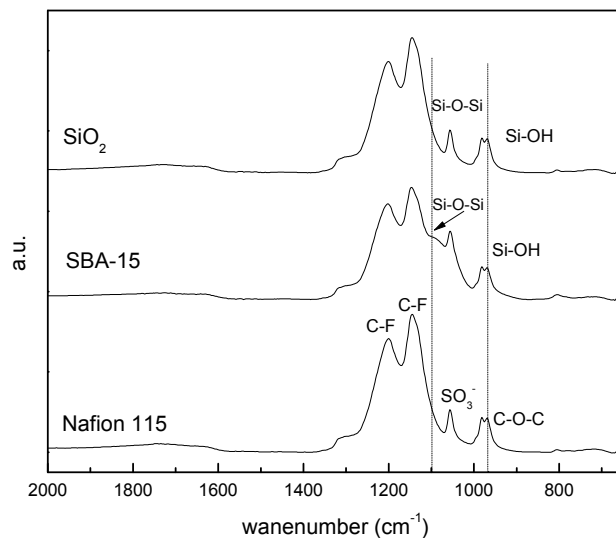


Figure 3. FT-IR spectra of Nafion® 115 and composite membranes.

metric vibration of Si-O-Si bonds. While the band at 463 cm<sup>-1</sup> is assigned to the torsion vibration of Si-O-Si, the band at 967 cm<sup>-1</sup> corresponds to the vibration of the Si-OH group. Also, the band at 1635 cm<sup>-1</sup> corresponds to free water, the intensive broad band centered at 3442 cm<sup>-1</sup> is assigned to the superposition of vibrations for both physically adsorbed H<sub>2</sub>O and silanol groups [21-23].

### 3.2. Physicochemical properties of composite membranes

FT-IR spectra in the wave number range 2000-400 cm<sup>-1</sup> of the composite membranes were recorded and are presented in Figure 3. The spectra indicate peak shifts in the composite membranes due to the presence of the fillers in the membrane structure. In the recast Nafion® membrane, the two major vibrational structures observed at 1199 cm<sup>-1</sup> and 1146 cm<sup>-1</sup>, correspond to the CF<sub>2</sub> stretching vibrations of the PTFE backbone. The peaks observed at 1055 and 967 cm<sup>-1</sup> are attributed to the stretching vibration moieties of SO<sub>3</sub><sup>-</sup> and C-O-C respectively [24]. The peak associated to the Si-O-Si bond is seen at 1063 cm<sup>-1</sup> while the SiOH stretching vibration in the composite membrane can be observed at 961 cm<sup>-1</sup>.

Water uptake and ionic exchange capacity of the composite membranes under study are shown in Table 2. Composite membrane SBA-15 has higher water uptake value than that obtained with Nafion® 115 membrane. Ion Exchange capacities IEC of

Table 2. Water uptake and ionic exchange capacity of composite membranes.

Membrane	Thickness / μm	Water Uptake / %	Ionic Exchange Capacity / mmol g <sup>-1</sup>
Nafion®115	127	25.67	0.9028
SiO <sub>2</sub>	180	29.72	0.7856
SBA-15	233	29.87	0.620

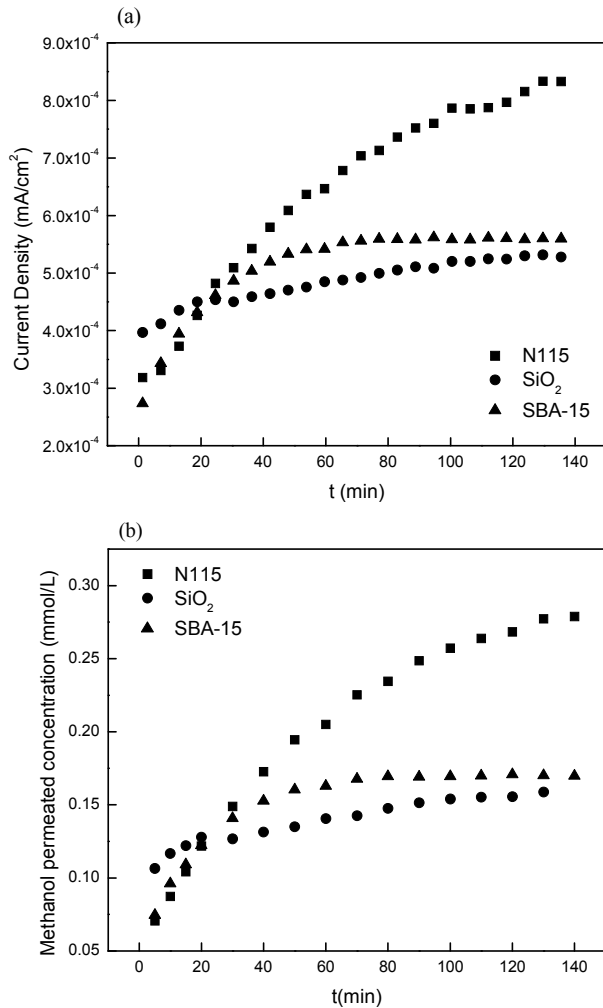


Figure 4. Methanol permeation rate curves of Nafion<sup>®</sup> 115 and composite membrane SiO<sub>2</sub> and SBA-15 at 25 °C. (a) Chronoamperometry plots, (b) Methanol permeation curves.

Nafion<sup>®</sup> 115 and composite membranes measured by titration, revealed that the IEC of the composite membranes diminished as a consequence of the presence of inorganic material [18, 25].

### 3.3. Electrochemical properties of composite membranes

Figure 4a shows the current vs time curves obtained as a result of the methanol permeation through the membrane. The composite film displays a lower permeability value than that obtained with the Nafion<sup>®</sup> 115. As expected, the concentration vs time curves (Figure 4b) also suggest that the use of these composite materials may have potential applications in DMFC. In this way, the methanol cross-over is reduced, this result suggest that the fillers have a blocking effect through the Nafion<sup>®</sup> channels, creating a tortuous path for the methanol passage [19].

Figure 5 also shows that the composite membranes have lower methanol permeability value (P) than that obtained when was used the Nafion<sup>®</sup> 115 membrane. Methanol permeability value (P) of

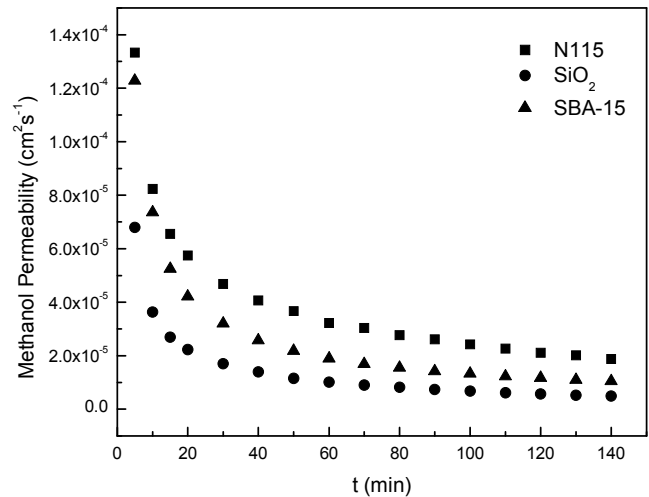


Figure 5. Methanol permeability rate curves of Nafion<sup>®</sup> 115 and composite membranes SiO<sub>2</sub> and SBA-15 (25 °C).

SiO<sub>2</sub>-based membrane corresponds to  $4.4 \times 10^{-6} \text{ cm}^2 \text{ s}^{-1}$  which is lower than that of Nafion<sup>®</sup> 115 membrane [10]. The composite membrane permeability SBA-15 on the other hand, corresponds to  $1.07 \times 10^{-5} \text{ cm}^2 \text{ s}^{-1}$  which is also lower than that obtained with Nafion<sup>®</sup> 115 ( $1.92 \times 10^{-5} \text{ cm}^2 \text{ s}^{-1}$ ). The composite membranes have lower methanol permeability (P), this result suggest that the inorganic fillers (SiO<sub>2</sub> and SBA-15) block the ion-exchange groups (sulfonic groups) in the polymeric matrix, creating a tortuous path for methanol (Table 3).

Polarization curves of the composite membranes are shown in Figure 6. The composite membranes reveal a better performance than that obtained for the Nafion<sup>®</sup> 115 membrane at the two temperature values surveyed (80 and 100 °C). At 80 °C the Nafion membrane has a similar behavior than that of the composite membranes, nevertheless, the better performance was obtained from the SiO<sub>2</sub> composite membrane with a power density value near of  $33 \text{ mW cm}^{-2}$ . At 100 °C, while the Nafion performance fell down around 50 %, the SiO<sub>2</sub> membranes improved their performance around 50 % with a maximum power density value that reached  $62 \text{ mW cm}^{-2}$  for SiO<sub>2</sub>, by SBA-15 membrane power performance was maintained in the value of  $29 \text{ mW cm}^{-2}$ .

## 4. CONCLUSIONS

This paper presents the characterization and evaluation of the methanol permeation of composite membranes prepared from a mixture of Nafion<sup>®</sup> 5% and 3% wt. of SiO<sub>2</sub> and SBA-15 fillers.

Table 3. Methanol permeability of Nafion<sup>®</sup> 115 and composite membranes (SiO<sub>2</sub> and SBA-15). Measurements at 25 °C.

Membrane	P /cm <sup>2</sup> s <sup>-1</sup> 3600s	P /cm <sup>2</sup> s <sup>-1</sup> 7200s	P /cm <sup>2</sup> s <sup>-1</sup> 8400s
N115	$3.22 \times 10^{-5}$	$2.11 \times 10^{-5}$	$1.88 \times 10^{-5}$
SiO <sub>2</sub>	$1.02 \times 10^{-5}$	$5.68 \times 10^{-6}$	$4.90 \times 10^{-6}$
SBA-16	$1.8 \times 10^{-5}$	$1.17 \times 10^{-5}$	$1.05 \times 10^{-5}$

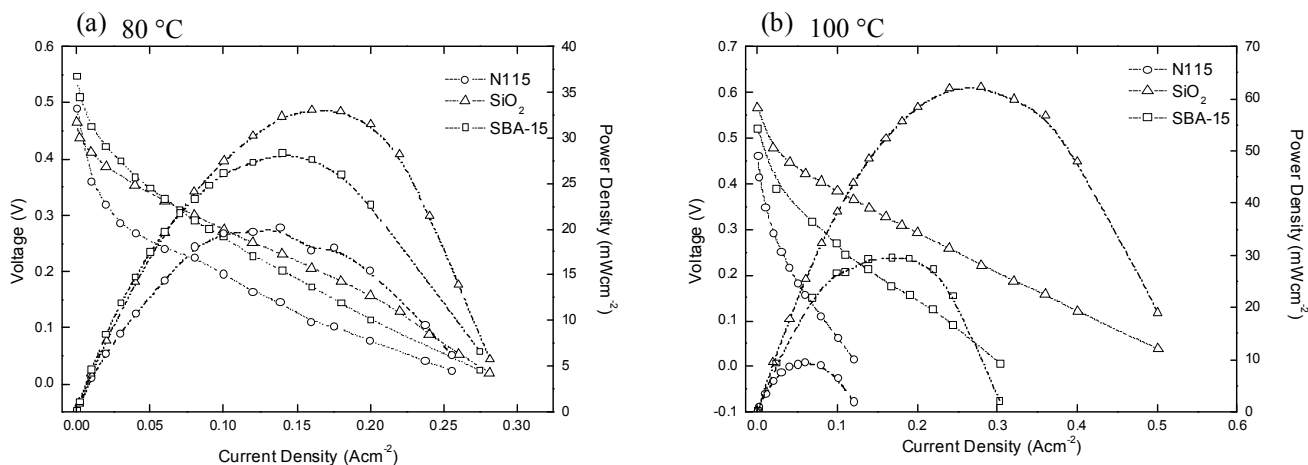


Figure 6. Polarization and power density curves for the various MEAs equipped with different membranes. At 80°C (a) and 100°C (b).

Composite membranes based in inorganic fillers showed a significant decrease in the concentration of methanol permeation, when were compared commercial Nafion® 115 membrane. Inorganic fillers (SiO<sub>2</sub> and SBA-15) could be hindering the passage of methanol by blocking exchange groups which reduces the permeation of alcohol.

## 5. ACKNOWLEDGEMENTS

A. Alvarez and C. Guzmán are grateful to Council for Science and Technology CONACYT for graduate fellowship. The authors thank the Mexican Council for Science and Technology for financial support through Fomix-Chihuahua Grant CHIH-2009-C02-127461 and SEP-CONACYT Grant 2009-133310.

## REFERENCES

- [1] V. Baglio, A.S. Aricò, A. Di Blasi, V. Antonucci, P.L. Antonucci, S. Licoccia, E. Traversa, F. Serraino Fiory, *Electrochim. Acta*, 50, 1241 (2005).
- [2] V. Baglio, A. Di Blasi, A.S. Aricò, V. Antonucci, P.L. Antonucci, F. Nannetti, V. Tricoli, *Electrochim. Acta*, 50, 5181 (2005).
- [3] W. Xu, T. Lu, C. Liu, W. Xing, *Electrochim. Acta*, 50, 3280 (2005).
- [4] R. Goslawit, S. Chirachanchai, S. Shishatskiy, S.P. Nunes, *Solid State Ionics*, 178, 1627 (2007).
- [5] C-Y Chen, J.I. Garnica-Rodriguez, M.C. Duke, R.F. Dalla Costa, A.L. Dicks, J.C. Diniz da Costa, *J. Power Sources*, 166, 324 (2007).
- [6] V. Neburchilov, J. Martin, H. Wang, J. Zhang, *J. Power Sources*, 169, 221 (2007).
- [7] S.W. Tay, X. Zhang, Z. Liu, L. Hong, S. Hwa Chan, *J. Membrane Sci.*, 321, 139 (2008).
- [8] C. Li, G. Sun, S. Ren, J. Liu, Q. Wang, Z. Wu, H. Sun, W. Jin, *J. Membrane Sci.*, 272, 50 (2006).
- [9] J. Wu, Z. Cui, C. Zhao, H. Li, Y. Zhang, T. Fu, H. Na, W. Xing, *Int. J. Hydrogen Energ.*, 34, 6740 (2009).
- [10] Y-F. Lin, C-Y Yen, C-C. Ma, S-H Liao, C-H Lee, Y-H Hsiao, H-P Lin, *J. Power Sources*, 171, 388 (2007).
- [11] J. González-Hernández, J.F. Pérez Robles, F. Ruiz, J.R. Martínez, *Sup. Vac.*, 1, 11 (2000).
- [12] R. Pérez-Hernández, J. Arenas-Alatorre, D. Mendoza-Anaya, A. Gómez-Cortés y G. Díaz., *Rev. Mex. Fís.*, 50, 80 (2008).
- [13] K. Flodstrom, V. Alfredsson, *Micropor. Mater.*, 59, 167 (2003).
- [14] R. Huirache-Acuña, B. Pawelec, E. Rivera-Muñoz, R. Nava, J. Espino, J.L.G. Fierro, *Appl. Catal. B-Environ*, 168, 92 (2009).
- [15] R. Nava, B. Pawelec, P. Castaño, M.C. Álvarez-Galván, C.V. Loricera, J.L.G. Fierro, *Appl. Catal. B-Environ*, 92, 154 (2009).
- [16] A.S. Aricò, V. Baglio, A. Di Blasi, P. Creti, P.L. Antonucci, V. Antonucci, *Solid State Ionics*, 161, 251 (2003).
- [17] S. Reichman, L. Burstein, E. Peled, *J. Power Sources*, 179, 520 (2008).
- [18] A. Saccà, I. Gatto, A. Carbone, R. Pedicini, E. Passalacqua, *J. Power Sources*, 163, 47 (2006).
- [19] Tao Li, Yong. Yang, *J. Power Sources*, 187, 332 (2009).
- [20] R.G. Rodríguez Avendaño, J.A. De Los Reyes, T. Viveros, J.A. Montoya De La Fuente, *Catal. Today*, 148, 12 (2009).
- [21] X. Feng, G.E. Fryxell, L.-Q. Wang, A.Y. Kim, J. Liu, K.M. Kemner, *Science*, 276, 923 (1997).
- [22] J. Liu, X. Feng, G.E. Fryxell, L.-Q. Wang, A.Y. Kim, M. Gong, *Chem. Eng. Technol.*, 21, 97 (1998).
- [23] C.E. Fowler, S.L. Burkett, S. Mann, *Chem. Commun.*, 1769 (1997).
- [24] V. Di Noto, R. Gliubizzi, E. Negro, G. Pace, *J. Phys. Chem. B*, 110, 24972 (2006).
- [25] G. Gnana Kumar, A.R. Kim, K. Suk Nahm, R. Elizabeth, *Int. J. Hydrogen Energ.*, 34, 9788 (2009).